Quantum Hall transitions in $(TMTSF)_2PF_6$

S. Valfells
Department of Physics, Boston University, Boston, Massachussets 02215

J. S. Brooks
Department of Physics, Boston University, Boston, Massachussets 02215
and Department of Physics, Florida State University, Tallahassee, Florida 32306-4005

Z. Wang*
Department of Physics, Boston University, Boston, Massachusetts 02215

S. Takasaki, J. Yamada, and H. Anzai
Himeji Institute of Technology, 2167 Shosya, Himeji, Hyogo 671-22, Japan

M. Tokumoto
Electrotechnical Laboratory, Tsukuba, Ibaraki 305, Japan
(Received 9 July 1996)

We have studied the temperature dependence of the integer quantum Hall transitions in the molecular crystal $(TMTSF)_2PF_6$. In the high-temperature regime, just below the transition temperature of the associated field-induced spin-density waves (FISDW), we find that the width of the transitions between the quantum Hall plateaus, as measured by the slope of the ρ_{xy} risers, $d\rho_{xy}/dB$, and the (inverse) width of the ρ_{xx} peaks, $(\Delta B)^{-1}$, decreases linearly with temperature; at low temperatures, however, the width saturates. We explain the temperature dependence of the width in terms of that of the order parameter of the FISDW and the characteristic impurity length scale of the system. [S0163-1829(96)04647-4]

One of the key features of the quantum Hall effect (QHE) in two-dimensional semiconductor heterostructures is the universal scaling behavior of the transitions between adjacent quantized Hall plateaus.[1] For the integer QHE, the maximum slope of the Hall step $(d\rho_{xy}/dB)$, and the half width of the ρ_{xx} peak (ΔB) scale as $(d\rho_{xy}/dB)^{-1} \sim \Delta B \sim T^{\kappa}$ with $\kappa \approx 0.42$.[1] This scaling behavior indicates that the quantum Hall transitions in semiconductor heterostructures are continuous zero-temperature phase transitions characterized by a single relevant length scale ξ_{loc}, the localization length, which diverges as $\xi_{\mathrm{loc}} \sim |\Delta B|^{-\nu}$ in the low-temperature limit. The localization of the electronic states, the resurrection of extended states at the center of the Landau levels, and the existence of scaling for the quantum Hall transitions as the Landau levels pass through the Fermi energy are intrinsic properties of a weakly disordered two-dimensional electron gas (2DEG) in a strong magnetic field.

Under quite different settings, the quantized Hall resistance plateau behavior has been convincingly demonstrated in the quasi-2D two-dimensional molecular crystals $(TMTSF)_2PF_6$ (Refs. 2 and 3) and $(TMTSF)_2ClO_4$.[4] In contrast to the case of 2DEG, the quantization of the Hall resistance in the organic crystals is due to the instability of the metallic open Fermi surface against spin-density-wave formation.[5] As pointed out by Poilblanc *et al.*[6] and Azbel, Bak, and Chaikin[7] the quantized Hall effect occurs as a result of the opening of a succession of gaps in the quasiparticle spectrum associated with the quantized nesting vectors of a series of magnetic-field-induced spin-density-wave (FISDW) states. The free energy of the system is at a minimum when the Fermi energy lies in one of the FISDW gaps which separate filled and empty Landau levels. Since the ordering wave vector changes discontinuously, the transitions between the FISDW subphases are first order. Consequently, the transitions between the quantized Hall plateaus are expected to be discontinuous *in the absence of impurities*. However, the precise nature and the properties of the FISDW generated quantum Hall transitions have not been investigated in the same way as in the better known quantum Hall effect in 2DEG systems. In this paper, we address this problem through the measured temperature dependence of the magnetoresistances in $(TMTSF)_2PF_6$. We find that $(\Delta B)^{-1}$ and $d\rho_{xy}/dB$, defined in a similar way as in the case of 2DEG, do not exhibit power-law scaling. Instead, they scale qualitatively as the square of the BCS-like, FISDW energy gaps.

$(TMTSF)_2PF_6$ (Refs. 8 and 9) is a highly anisotropic conductor: parallel chains of the TMTSF molecules form planes separated by the PF_6 complex, with transfer integral values of t_a (along the chains), t_b (between adjacent, coplanar chains), and t_c (between planes) approximately equal to 300, 30, and 1 meV, respectively. At ambient pressure, $(TMTSF)_2PF_6$ undergoes a spin-density-wave (SDW) transition at $T_{\mathrm{SDW}} \approx 12$ K, but when pressurized, it becomes superconducting at pressures in excess of $P_c \approx 8$ kbar with $T_c \approx 1$ K.[10] In a magnetic field ($B\|$ to the c axis) and at $P > P_c$, $(TMTSF)_2PF_6$ exhibits a succession of FISDW's. These are explained[5,11] by the nesting of the slightly warped, one-dimensional Fermi surface (Fig. 1) through a succession of field-dependent nesting vectors with a quantized component along the stacking direction: $Q_a = 2k_F + NeBb/\hbar$. The phase

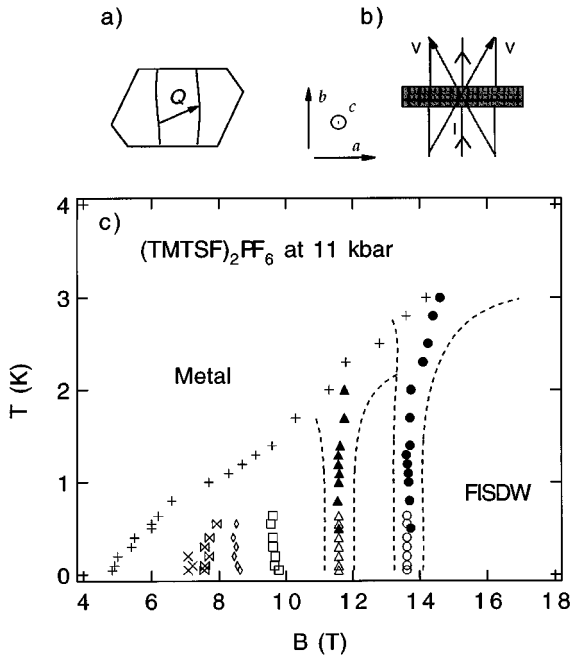

FIG. 1. Overview of $(TMTSF)_2PF_6$. (a) Fermi surface of $(TMTSF)_2PF_6$ with nesting vector Q. [Coordinates refer to both (a) and (b)]. (b) Lead configuration of the sample. (c) Phase diagram at 11 kbar. +,mark metallic—FISDW second-order phase boundary. $\times$, $\bowtie$, $\diamond$, $\square$, $\triangle$, and $\circ$: Hall transitions $n_H=7\rightarrow6$, $6\rightarrow5$, $5\rightarrow4$, $4\rightarrow3$, $3\rightarrow2$, $2\rightarrow1$, respectively. The regions delimited by the broken lines represent the widths of the lowest two transitions. Open symbols and closed symbols correspond to low- and high-temperature experimental runs and field sweep rates of 0.33 T/min and 1.02 T/min, respectively.

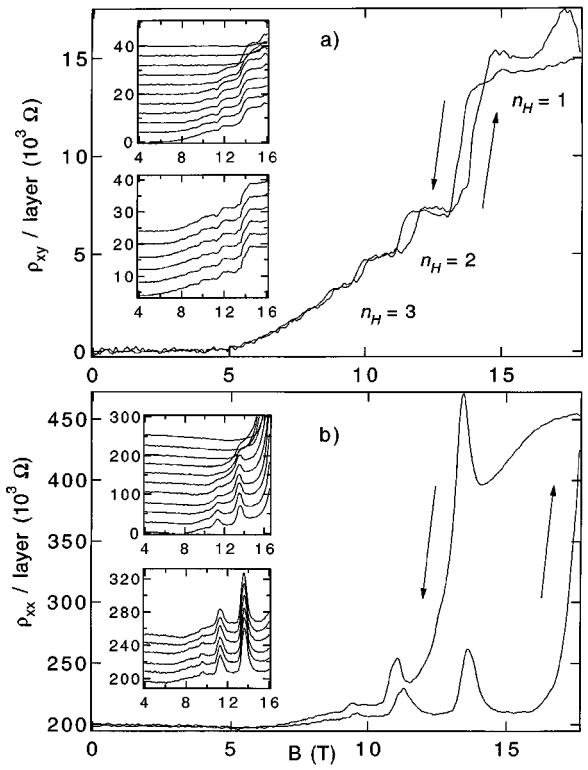

FIG. 2. (a) Hall resistivity. Main trace: complete field sweep at 50 mK. Transition steps $n_H=1$, 2, and 3 are indicated. Insets are upsweeps only, offset from zero for clarity. Upper inset: 4.2, 3.0, 2.3, 1.7, 1.4, 1.3, 1.2, 1.1, 1.0, 0.8, 0.5 K. Lower inset: 640, 550, 400, 300, 200, 100 mK. (b) Longitudinal magnetoresistivity. Main trace: complete field sweep at 50 mK. Insets are upsweeps only, offset from zero for clarity. Sequence of temperatures is the same as in (a). Note the significant difference in hysteretic behavior of ρ_{xx} compared with that of ρ_{xy}.

diagram of our $(TMTSF)_2PF_6$ sample at 11 kbar is shown in Fig. 1. The second-order transition line separates the metallic and the FISDW phases, whereas different FISDW phases are separated by the nearly vertical phase boundaries where the quantized Hall plateau transitions take place. In an ideal sample without impurities, the latter transitions are sharp and first order in nature, and the corresponding Hall plateau transitions are discontinuous. However, in realistic samples where impurities are always present, the transitions are broadened and their widths (delimited by the broken lines in Fig. 1) saturate at low temperatures.

Six gold leads were attached to the sample on the edge perpendicular to the b axis, three on each side as shown in Fig. 1. The sample was then pressurized in a BeCu cell with a fluorocarbon fluid. A standard ac lock-in technique, with a current of 10 μA, was used to acquire the data. The Hall signal ρ_{xy} (ρ_{xx} signal) was obtained by subtracting (adding) constant temperature field sweeps of opposite polarity. Results at low temperatures (50–640 mK) were obtained in a dilution refrigerator and a 20 T superconducting magnet. Higher-temperature measurements (0.5–4.2 K) were done in a ^{3}He cryostat and a 30-T resistive magnet.

The ρ_{xy} and ρ_{xx} data are shown in Fig. 2. The gross features are consistent with the QHE phenomenology in 2DEG: Hall plateaus in ρ_{xy} are evident, as are the pronounced Shubnikov–de Haas oscillations in ρ_{xx} with minima coinciding with the location of the ρ_{xy} plateaus. Nevertheless, there are obvious differences.[2,3] Since the prerequisite for observing Hall resistance quantization in $(TMTSF)_2PF_6$ is the opening of quasiparticle gap in the FISDW phases, the Hall signal is zero until the sample enters the FISDW phase. This should be contrasted to the conventional integer QHE in 2DEG that requires a ''mobility gap'' provided by disorder-induced localization of electronic states at the Fermi energy away from the band centers. Consistent with previous workers,[2,3] we treat the sample as a sandwich of N parallel 2D layers; and by measuring the thickness of the sample along the c axis, we can estimate the number of parallel 2D layers and calculate the resistivity per layer. Our measurements yield a resistivity value of 13.0 ± 1.5 kΩ per layer at the $n_H=1$ plateau. This value is consistent with the expected value of $h/2e^2$ (12.9 kΩ) per layer as a result of the unresolved spin degeneracy factor of two in the FISDW. We note the absence of negative ''Ribault'' Hall steps seen in earlier measurements.[2] Negative Hall steps seem to occur in the low-pressure regime[13] ($P\approx8$–9 kbar) just above P_c. Our value of $P\approx11.3\pm0.5$ kbar is well above P_c.

The transitions have a frequency of $B_1=67\pm7$ T, which is consistent with the values previously reported.[2,3] The FISDW transitions are predicted to occur at the zeros of the Bessel function $J_0(x)$, $x=2ct_b'/veBb$ (v is the Fermi velocity; t_b' is the next-nearest-neighbor tight-binding transfer

energy).[5] Consequently, the data can be used to estimate t_b'. To first approximation, v scales as $(b)^{-1}$, and, vb stays roughly constant when the sample is pressurized. Using the ambient pressure values $v \approx 10^7$ cm/s and $b \approx 7.7$ Å, we find that $t_b' \approx 5$ meV, which meets the criterion $t_b' \ll t_b$. Fitting our data to the ''standard model'' expression[15] $B_{n_H} = B_1/(\gamma + n_H)$ for the higher transitions labeled by n_H as in Fig. 2 yields $\gamma = 2.9$. The latter value corresponds to $t_b'/t_b \approx 1/10$ in good agreement with the estimate above based on the value of B_1, especially if one takes into account the fact that t_b should increase with pressure.[15]

In analogy to the integer quantum Hall transitions in 2DEG, the ρ_{xx} signal (Fig. 2) peaks at the transitions between the Hall plateaus. We draw attention to the large amplitude of the ρ_{xx} peaks and the small magnetoresistance background. The low background magnetoresistance within the Hall plateau–FISDW phases is indicative of a (relatively) low sample impurity content. Indeed, as pointed out by Azbel, Bak, and Chaikin,[7] the effects of impurities on the QHE induced by the FISDW differ significantly from those in the conventional integer QHE in 2DEG. While in the latter disorder provides localization of the electronic states and, consequently, the absence of dissipation necessary for observing the QHE, in the present case, impurities introduce extended states in the FISDW gap and give rise to finite ρ_{xx} and nonintegral values of the ρ_{xy} plateaus. Over the entire range of our measurements, the sample resistivity was in the residual resistivity limit (temperature independent) as shown in Fig. 3.

We turn now to the question of how impurities affect the transition between the quantized Hall plateaus. Our main results are the temperature dependence of the Hall risers $(d\rho_{xy}/dB)$, the half width of the ρ_{xx} peaks (ΔB), and the peak value $(\rho_{xx}^{\max})$, which are shown in Fig. 3. ΔB and $(d\rho_{xy}/dB)^{-1}$ independently measure the width of the transition between two FISDW phases of filled Landau levels in the same manner as in the QHE in semiconductors. Figures 3(a) and 3(b) clearly show that they do not exhibit power-law scaling with temperature: instead, the temperature dependence of each resembles more that of the BCS-like FISDW gaps (apart from the finite slope at $T \approx T_c$), and saturates to a finite value at low temperatures. Thus, the transition width is finite as indicated in the phase diagram (Fig. 1). In fact, the low-temperature data are consistent with the transitions taking place through certain intervening metallic phases stabilized, presumably, by disorder. To a first approximation in the transition region, let us consider the simple Drude expressions: $(\rho_{xy}, \rho_{xx}) = (B/n_{\text{eff}}ec, m/n_{\text{eff}}e^2\tau)$, where $n_{\text{eff}}(T)$ is the effective carrier concentration and τ is a temperature-independent impurity scattering time. $d\rho_{xy}/dB$ therefore measures the T dependence of the inverse carrier concentration near the transition. The dissipative resistance, ρ_{xx}, in the transition region should then follow the same temperature dependence, with overall magnitude oscillating with the magnetic field. This is supported by Fig. 3(c) where the normalized peak values $\rho_{xx}^{\max}/\rho_0$ indeed scale approximately with n_{eff}^{-1}.

In the original work of Gor'kov and Lebed,[5] an oscillatory phase diagram between the FISDW subphases and the metallic state was predicted, which would imply reentrant metallic behavior even in pure systems. Since the carrier concentration in the metallic phase would be temperature independent, it should also be so in the transition regions in the data, and the Hall signal would drop to some constant value in these regions. Instead, the carrier concentration seems to follow the SDW gap behavior for any field above the threshold field for the FISDW.

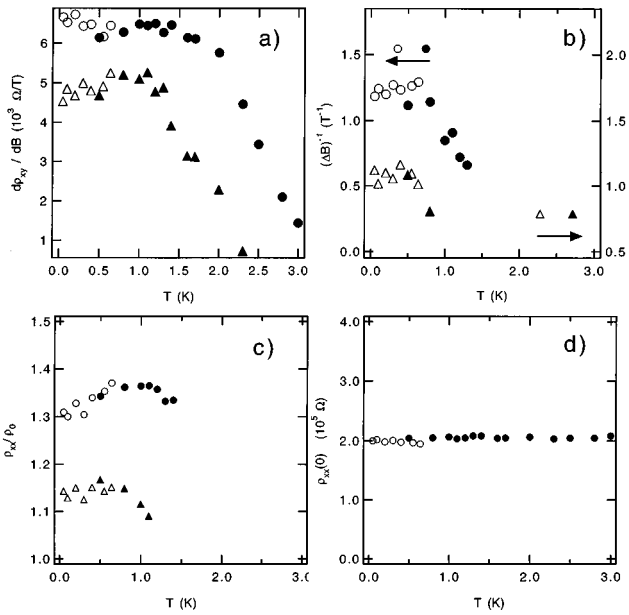

FIG. 3. Temperature dependence of resistivity and Hall transition parameters. In all cases, circles mark the 2→1 transition and triangles the 3→2 transition. Open symbols and closed symbols correspond to low- and high-temperature experimental runs and field sweep rates of 0.33 and 1.02 T/min, respectively. (a) Scaling of the Hall transitions. $d\rho_{xy}/dB$ is estimated by the slope of the riser as obtained by linear interpolation. The broken line represents the temperature dependence of the square of the BCS gap, Δ_{BCS}^2, fitted to the 2→1 transition. In the graph, we use $T_c = 3.0$ K (Δ_{BCS}^2 fits well over the range $2.9 \leqslant T_c \leqslant 3.3$ K). The zero-temperature gap amplitude is normalized to the value of $d\rho_{xy}/dB$ at $T = 0$ K (Ref. 16). The magnetoresistance peak width. The width of the transition, ΔB, is estimated by the full width at half maximum of a Lorentzian fit to the peaks. (c) The magnetoresistance peak amplitude (normalized to the zero-field residual resistivity). (d) Zero-field residual resistivity of ρ_{xx} as a function of temperature.

Our data strongly suggest that the finite transition width (within which there is metallic behavior) is a consequence of the broadening of the first-order transition in ideal systems by disorder effects. Let w be the width of the transition between two adjacent subphases with gap order parameters Δ_{n+1} and Δ_n. Thus $w \sim (d\rho_{xy}/dB)^{-1} \sim \Delta B$ in the transition region. In the absence of impurities, the transitions between the FISDW's are discontinuous in the thermodynamic limit. For a finite system of linear dimension L, it is well known that the rounding of the critical singularities in a first-order transition leads to a transition width that scales with L^{-d} where d is the effective dimensionality of the system.[13] Denoting the coherence length by ξ which remains finite at a first-order transition, then $w \propto 1/(L/\xi)^d$. In the presence of a disorder potential that couples to the FISDW order parameter (e.g., through lattice distortions), the stability of the first-

order transition has to be considered. The essential physics can be captured by the Imry-Ma argument:[14] it is energetically favorable for the system to form domains over which there is a single phase. The typical size of the domains is given by the Imry-Ma length scale, $L_{\rm im}$, which is determined by the impurity strength and the detailed competition between the interfacial domain-wall energy cost and the bulk energy gain. The important point is that the free energy of the system is the sum of the free energies of the domains (with corrections due to the nonextensive contributions from the domain-wall energies), and is identified with its disorder average over domains of size $L_{\rm im}$. Consequently, $L_{\rm im}$ plays the role of the effective finite size of the system. The coherence length is related to the gap parameter through $\xi \sim \hbar \overline{v}/\Delta$, where Δ is an averaged gap order parameter for the two adjacent FISDW subphases (Δ_n and Δ_{n+1}) and $\overline{v}$ is an averaged Fermi velocity. The transition width is therefore $w \propto (\hbar v/L_{\rm im}\Delta)^d$. For our quasi-two-dimensional system, we take $d \approx 2$, and w^{-1} should then scale as the square of the BCS-like FISDW gap parameters, which is consistent with the observed temperature dependence of $d\rho_{xy}/dB$, $(\Delta B)^{-1}$, and $\rho_{xx}^{\rm max}/\rho_0$ in Fig. 3.

Specifically, on approaching the second-order phase-transition line between the metal and the FISDW in Fig. 1, i.e., near T_c, $\Delta \approx \Delta_c(1-T/T_c)^{1/2}$ and $w^{-1} \sim 1-T/T_c$, which explains the linear behavior around T_c in Fig. 3. In the low-temperature limit, on the other hand, $\Delta \approx \Delta_0 - (2\pi\Delta_0 T)^{1/2} e^{-\Delta_0/kT}$, and the BCS-like gap saturates exponentially regardless of the dimensionality; consequently, w is limited by $L_{\rm im}$. Since the residual resistivity is constant over the range of temperatures of interest in the present experiment [Fig. 3(d)], we take $L_{\rm im}$ to be constant. Consequently, as observed in Fig. 3, w^{-1} is constant in the low-temperature limit. Finally, as the field sweeps away from transition region, bulk FISDW order will take place, which is presumably assisted initially by the quantum tunneling between the domains of the prevailing phase.

This research is supported by NSF DMR 95-10427. Experiments were carried out at the National High Magnetic Field Laboratory (supported by the NSF and the State of Florida). We acknowledge A. Lacerda, E. Palm, T. Murphy, and M. Davidson for technical assistance, and N. Bonesteel, C. Campos, L. P. Gor'kov, V. Melik-Alaverdian, P. Sandhu, and S. Uji for useful discussions.

*Present address: Department of Physics, Boston College, Chestnut Hill, MA 02167.

[1] H. P. Wei, D. C. Tsui, M. A. Paalanen, and A. M. M. Pruisken, Phys. Rev. Lett. **61**, 1294 (1988).

[2] J. R. Cooper, W. Kang, P. Auban, G. Montambaux, and D. Jérôme, Phys. Rev. Lett. **63**, 1984 (1989).

[3] S. T. Hannahs, J. S. Brooks, W. Kang, L. Y. Chiang, and P. M. Chaikin, Phys. Rev. Lett. **63**, 1988 (1989).

[4] P. M. Chaikin, M. Y. Choi, J. F. Kwak, J. S. Brooks, K. P. Martin, M. J. Naughton, E. M. Engler, and R. L. Greene, Phys. Rev. Lett. **51**, 2333 (1981); M. Ribault, D. Jérôme, J. Tuchendler, C. Weyl, and K. Bechgaard, J. Phys. (Paris) Lett. **45**, L985 (1984); M. Ribault, Mol. Cryst. Liq. Cryst. **119**, 91 (1985).

[5] L. P. Gor'kov and A. G. Lebed, J. Phys. (Paris) Lett. **45**, L433 (1984).

[6] D. Poilblanc, G. Montambaux, M. Hértier, and P. Lederer, Phys. Rev. Lett. **58**, 270 (1987).

[7] M. Ya. Azbel, P. Bak, and P. M. Chaikin, Phys. Rev. Lett. **59**, 926 (1987).

[8] For a review, see T. Ishiguro and K. Yamaji, *Organic Superconductors* (Springer-Verlag, Berlin, 1990).

[9] W. Kang, S. T. Hannahs, and P. M. Chaikin, Phys. Rev. Lett. **70**, 3091 (1993).

[10] Pressure at room temperature. Pressure is reduced by 2–3 kbar at liquid-helium temperatures. See J. Thompson, Rev. Sci. Instrum. **55**, 232 (1984).

[11] G. Montambaux and D. Poilblanc, Phys. Rev. B. **36**, 1913 (1988). A.

[12] L. Balicas, G. Kriza, and F. I. B. Williams, Phys. Rev. Lett. **75**, 2000 (1995).

[13] M. E. Fisher and A. N. Berker, Phys. Rev. B **26**, 2507 (1982).

[14] Y. Imry and S.-K. Ma, Phys. Rev. Lett. **35**, 1399 (1975).

[15] G. Montambaux, M. Hértier, and P. Lederer, J. Phys. C **19**, L293 (1986).

[16] B. Mühlschlegel, Z. Phys. **155**, 313 (1959).